

FORECAST OF HEAT TRANSFER USING A COMPUTATIONAL FLUID DYNAMICS ANALYSIS(CFD)

Purushotama Anil Kumar Pilla
Student(M.Tech) , Mechanical Dept
Gokul group of institutions
Visakhapatnam, India

Vommi Pradeep Kumar
ASSOCIATE PROFF, Mechanical Dept
Gokul group of institutions
Visakhapatnam, India

Abstract— The aim of this project was to the current state of heat transfer forecasting for commonly used CFD software. FINE/Turbo code is used for this software since it has a time accurate advantage. The computational model utilized a conjugate heat-transfer model for solid-fluid interactions with the turbine blade hardware. Current heat-transfer solutions are in the expected range of theoretical values, although the measurement program is still in process. Due to addition of cooling flow to the mainstream flow associated with a high-pressure turbine stage is difficult to model, especially when one is attempting to predict the surface heat-transfer rate. Boundary layer conditions and solid-fluid interactions dominate the region, making accurate computational predictions very difficult. Results of this project have identified areas for which improvement in the current state-of-the-art are required, and have provided a benchmark for computational solutions. Lessons learned from the flat-plate measurement program will be applied to a full-scale rotating turbine stage in the near future, so understanding how to predict the local heat transfer using the CFD code is of major one.

Keywords—Heat Transfer Computational Fluid Dynamics.

I. THE RESEARCH PROGRAM AND BACKGROUND INFORMATION

1.1 Introduction to Turbine Cooling

The dramatic increase of computing power in the last 20 years has revolutionized thermal and fluid science, paving the way for full-scale turbine simulations using Computational Fluid Dynamics. CFD predictions of turbine aerodynamics have recently become quite accurate, allowing for a quicker and more robust design of jet engine turbines [2]. Predicting heat transfer for film-cooled turbines, however, remains a difficult and arduous task, which continues to slow and hamper turbomachine development. Compounding this dilemma is the industry's ceaseless drive to increase engine efficiency, primarily accomplished by raising the inlet temperature of hot gasses to the turbine from the combustor [3]. In many applications, inlet temperatures are at or above the melting point of the metal from which the turbine blades are constructed. Moreover, combustor

exit non-uniformities such as turbulence and hot streaks can lead to unbalanced heat loads in the turbine, resulting in high levels of thermal stresses ultimately ending in blade failure [4]. In order to avoid catastrophic thermal failure in the turbines, a variety of innovative techniques have been employed, including coating turbine airfoils with special thermal barriers and introducing a thin film of coolant air over the airfoils for protection from the devastating effects of hot combustion gasses [5]. This addition of coolant air has become common practice in high-performance engines, but since the air is traditionally extracted from the compressor stage, a decrease in thermodynamic cycle efficiency results [6]. Thus, it is advantageous to bleed only the optimal amount of air in order to maintain efficiency while still cooling the airfoils.

II. EXPERIMENTAL SETUP

2.1 Small Calibration Facility

The CFD simulations of this project were designed to model the real-world experiments conducted in the Small Calibration Facility (SCF) at the OSU GTL. A short description of the SCF and its operation has been included to provide some background information. The SCF operates as a medium-duration blow-down facility, which is used for both instrument calibration and as a small test facility [5]. In this experimental investigation, the SCF was utilized in its small test facility capacity. A photograph of the SCF and a schematic are included below as Figures 1 and 2.



Figure 1: Photograph of the Small Calibration Facility

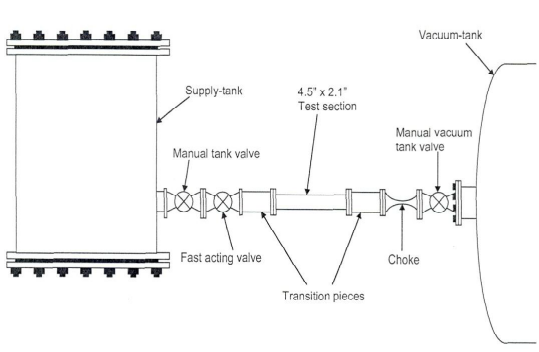


Figure 2: Schematic of the Small Calibration Facility [5]

The SCF runs as blow-down wind tunnel, with subsonic flow through the 4.5” x 2.1” test section, flow of Mach 1 at the choke, and supersonic flow on the vacuum-tank side of the choke. A 0.71 m³ supply tank provides heated and pressurized air to the test section, where the instrumented flat-plate used in the experiment is located. The air inside the supply tank is mixed using an internal fan, and is insulated from the outside with fiberglass insulation. Thus, the air inside the supply tank can be considered homogenous in both temperature and pressure.



Figure 3: Test Section Containing Flat Plate

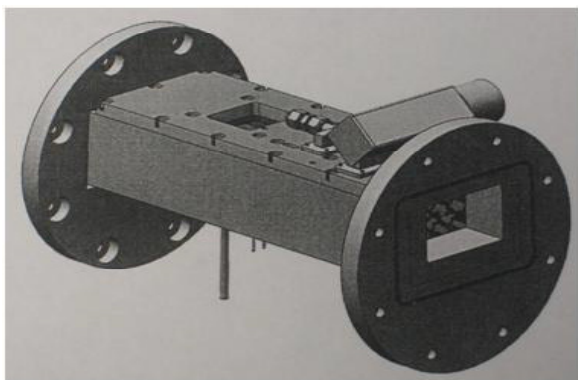


Figure 4: CAD Model of the Test Section [5]

2.2 Boundary Conditions

The boundary conditions used in the CFD simulations were modeled after the flat plate experiments of the SCF. Table 2.1 summarizes the given boundary conditions, while Table 2.2 shows the boundary conditions that required further calculations using the given values.

Table 1: Given Test Section Boundary Conditions

| | | |
|-------------|------------------------------|------------|
| Ma | Inlet Mach Number | 0.4 |
| T_s | Inlet Static Temperature | 470 K |
| T_{cool} | Cooling Gas Temperature | 240 K |
| P_s | Supply Tank Pressure | 517.1 kPa |
| \dot{m}_c | Cooling Mass Flow | 0.006 kg/s |
| k_{al} | 6061-T6 Thermal Conductivity | 177 W/mK |

Table 2: Calculated Test Section Boundary Conditions

| | | |
|-------------|-----------------------------|------------|
| c | Speed of Sound | 433 m/s |
| V | Flow Velocity | 173 m/s |
| P_o | Outlet Pressure | 463.13 kPa |
| \dot{m}_a | Air Mass Flow (theoretical) | 3.66 kg/s |

The Mach number, supply tank pressure, cooling gas temperature, and inlet temperature were provided for this experiment. The cooling mass flow and thermal conductivity were also assumed to be given values in this experiment. However, difficulties were encountered in determining the thermal conductivity of the flat plate. It was known that the plate was made out of aluminum, likely of the 6000 series. However, the exact aluminum alloy used was not known, since it was never specified to the machine shop that created the flat plate.

Table 3: Heat Transfer Calculation Properties

| | | |
|------------|--------------------------|------------------------|
| ρ | Air Density | 1.21 kg/m ³ |
| L | Plate Length | 0.289 m |
| μ | Dynamic Viscosity | 2.26 E-5 kg/ms |
| Pr | Prandtl Number | 0.70 |
| k_{air} | Air Thermal Conductivity | 0.0321 W/mK |
| ΔT | Temperature Difference | 170 K |

III. COMPUTATIONAL FLUID DYNAMICS

3.1 Introduction

The FINE/Turbo software family handled all of the computational processes of this research, from grid generation and processing to post-processing. By keeping all computational activities within a single software package, the difficulties of moving from one platform to another were completely eliminated. All computations were carried out using a dual-core Intel Xenon processor, with each core running at a clock speed of 2.99 GHz. Although the GTL has a 16-node SGI cluster available for major computational activities, it could not be utilized for this project. A basic understanding of blocks in FINE/Turbo is required to why this was the case.

3.2 Preprocessing: IGG

The first step towards the successful completion of any CFD analysis is the accurate modeling of the relevant geometry. In order to accomplish this, detailed dimensions of the SCF and flat plate were taken. In addition, the leading edge of the flow model was assumed to start at the boundary layer bleed plate. This plate resets the boundary layer upstream of the cooled flat plate, removing the preformed boundary layer. The exit of the model was set at the trailing edge of the flat plate vane piece. Final dimensions for the computational model are shown in Table 4 below.

Table 4: Numerical Model Dimensions

| | Length (m) | Width (m) | Height (m) |
|------------|------------|-----------|------------|
| Flat Plate | 0.289 | 0.114 | 0.0237 |
| Air Flow | 0.289 | 0.114 | 0.0536 |

Table 5: Multigrid Levels for 129 Points

| Multigrid level | X Grid Points | Y Grid Points | Z Grid Points |
|-----------------|---------------|---------------|---------------|
| 1 | 2 | 2 | 2 |
| 2 | 3 | 3 | 3 |
| 3 | 5 | 5 | 5 |
| 4 | 9 | 9 | 9 |
| 5 | 17 | 17 | 17 |
| 6 | 33 | 33 | 33 |
| 7 | 65 | 65 | 65 |
| 8 | 129 | 129 | 129 |

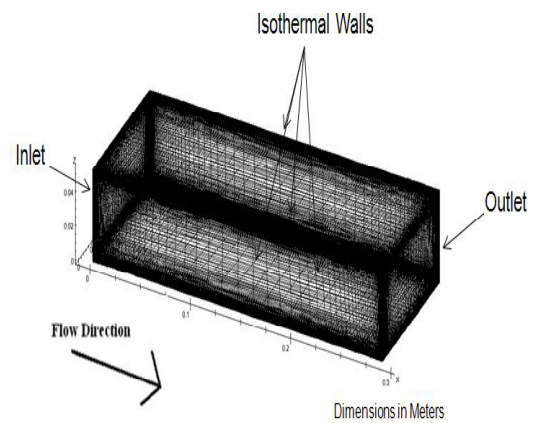


Figure 5: Single Block Wall Boundary Conditions

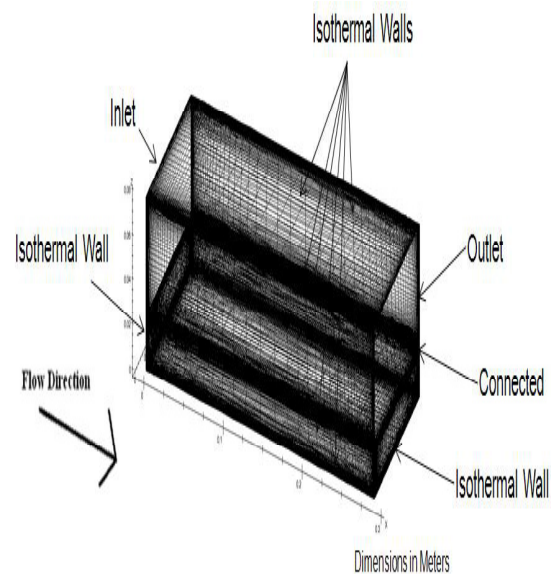


Figure 6: Two Block Wall Boundary Conditions

IV. RESULTS

4.1 Single Block Results

Although the single block CFD mesh was relatively simple in nature, it was still able to provide a useful prediction of flat plate heat transfer. Figure 11 shows a color map of the heat transfer for the single block case. Relevant boundary conditions from Tables 1 and 2 are repeated in Table 7 below for ease of reference.

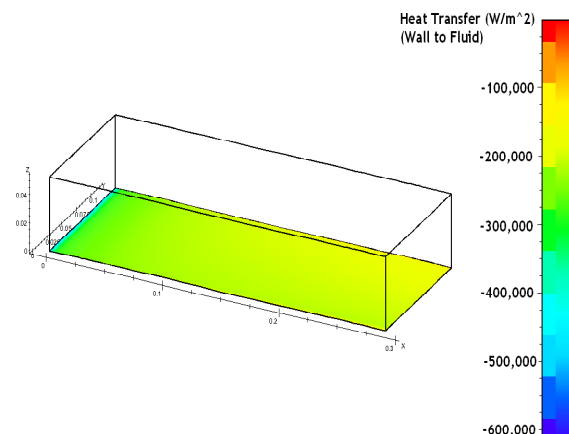


Figure 7: Uncooled Single Block Heat Transfer

| | | |
|------------|--------------------------|------------|
| Ma | Inlet Mach Number | 0.4 |
| T_s | Inlet Static Temperature | 470 K |
| V | Flow Velocity | 173 m/s |
| P_o | Outlet Pressure | 463.13 kPa |
| T_{wall} | Wall Temperature | 300 K |
| m_c | Cooling Mass Flow | 0.006 kg/s |
| T_{cool} | Cooling Gas | 240 K |

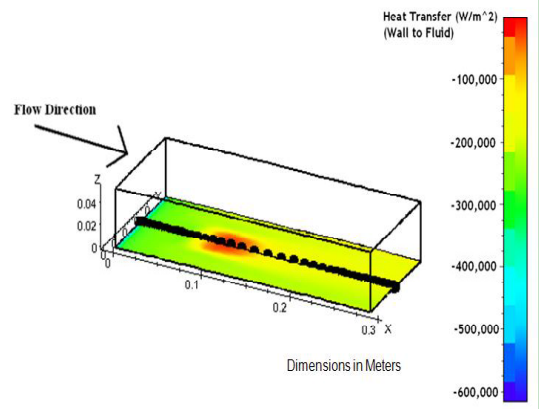


Figure 11: Cooled Single Block Gauge Location

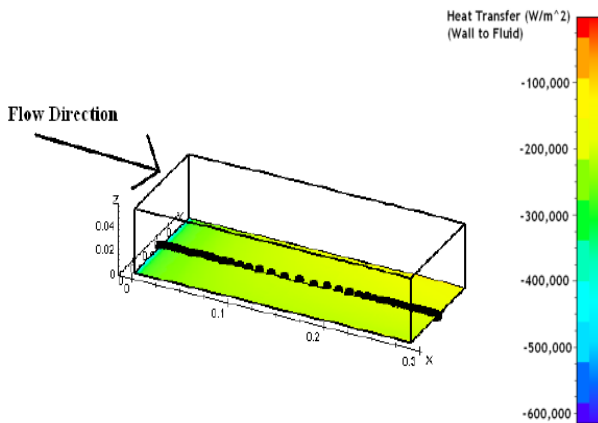


Figure 8: Uncooled Single Block Gauge Location

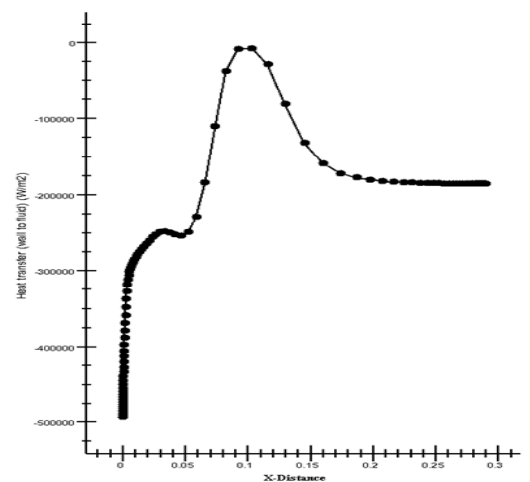


Figure 12: Cooled Single Block Heat Transfer Graph

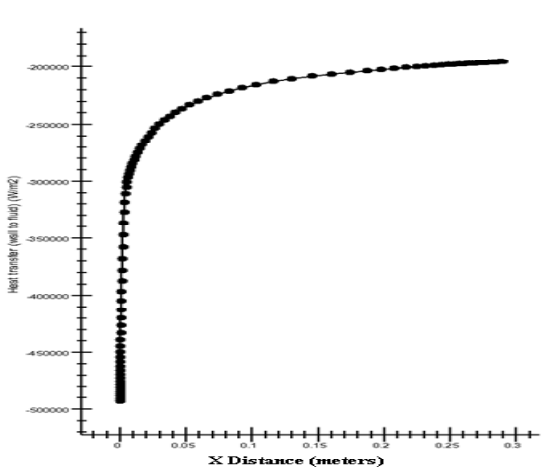


Figure 9: Uncooled Single Block Heat Transfer Graph

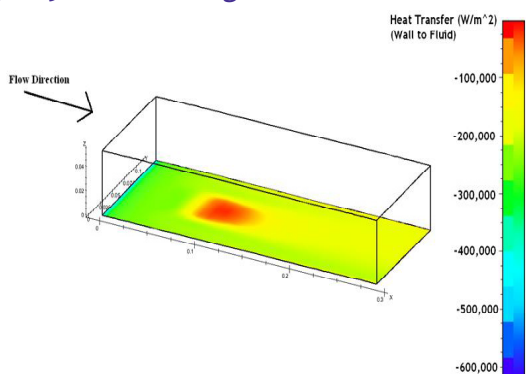


Figure 10: Cooled Single Block Heat Transfer

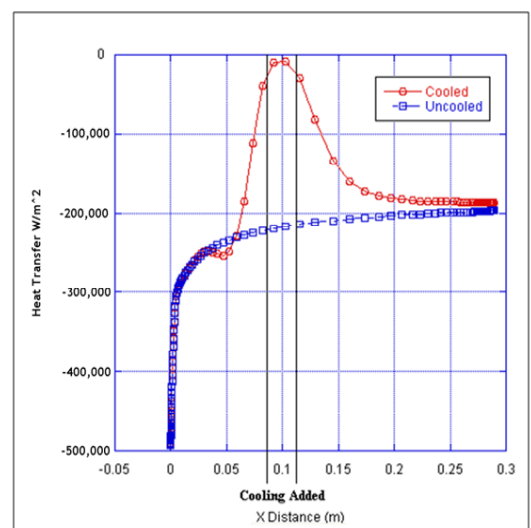


Figure 13: Comparison of Single Block Cooled and Uncooled Heat Transfer

The heat transfer is the same for both the cooled and uncooled plates upstream of the cooling holes, as expected. The addition of cooling gas has no effect on heat transfer at the leading edge. Moving downstream, adding cooling gas initially caused the heat transfer to increase before rapidly dropping off. The reason for this is uncertain. Additionally, this unusual result was obtained even when the mass flow of the cooling gas was increased by a factor of 5, so the behavior does not appear to be dependent on the amount of cooling mass flow.

CONCLUSION

In conclusion, CFD predictions for the experimental flat plate were obtained in this research effort. Although experimental data is still in work and is unfortunately unavailable, computational predictions were compared with the theoretical value from forced convection heat transfer equations. The single block CFD model predicted a steady heat transfer of 196 kW/m² with a developed boundary layer. Since the theoretical value for a fully developed turbulent boundary layer was 186 to 195 kW/m², the CFD heat transfer predictions appear to be reasonable. Moreover, the single block mass flow of 3.64 kg/s compares well with the theoretical mass flow of 3.66 kg/s.

REFERENCES

- [1] Dunn, M. G., 2001, "Convective Heat Transfer and Aerodynamics in Axial Flow Turbines," ASME Journal of Turbomachinery, Vol. 123, pp. 637-686.
- [2] Haldeman, C. W., Mathison, R. M., Dunn, M. G., Southworth, S., Harral, J. W., and Heitland, G., 2006, "Aerodynamic and Heat Flux Measurements in a Single Stage Fully Cooled Turbine- Part I: Experimental Approach," ASME Paper No. GT2006-90966.
- [3] Haldeman, C. W. and Dunn, M. G., 2003, "Heat Transfer Measurements and Predictions for the Vane and Blade of a Rotating High-Pressure Turbine Stage," ASME Paper No. GT2003-38726.
- [4] Varadarajan, K. and Bogard, D. G., 2004, "Effects of Hot Streaks on Adiabatic Effectiveness for a Film Cooled Turbine Vane," ASME Paper No. GT2004-54016.
- [5] Bernasconi, S.L., 2007, "Design, Instrumentation and Study on a New Test Section for Turbulence and Film Effectiveness Research in a Blowdown Facility". M.S. Thesis, ETH Zurich.
- [6] Ou, S. and Rivir, R. B., 2006, "Shaped-Hole Film Cooling With Pulsed Secondary Flow," ASME Paper No. GT2006-90272.
- [7] Giang, T. T. L., 1999, "Effects of Unsteady Cooling Flow on Heat Transfer to a Film-Cooled Flat Plate," M.S. Thesis, The Ohio State University.
- [8] Lienhard, J. H. and Lienhard, J. H., 2008, A Heat Transfer Textbook, Cambridge, MA: Phlogiston Press.
- [9] Anon., 1953, "Equations, Tables, and Charts for Compressible Flow," NACA rept. 1135.
- [10] Incropera F.P. and DeWitt, D. P., 2002, Fundamentals of Heat and Mass Transfer, New York: Wiley.
- [11] Crosh, E. A., 2008, "Time-Accurate Predictions for the Aerodynamics of a 1 and ½ Stage HP Transonic Turbine," M.S. Thesis, The Ohio State University